Contribution from the Department of Chemistry,
University of Minnesota, Minneapolis, Minnesota 55455

Synthesis and Interconversions of Several Tri- and Tetranuclear Ruthenium Isocyanato Carbonyl Clusters. Crystal and Molecular Structure of $H_3Ru_4(NCO)(CO)_{12}$

DOUGLAS E. FJARE, JAMES A. JENSEN, and WAYNE L. GLADFELTER*

Received October 6, 1982

The reaction of $Ru_3(CO)_{12}$ with $PPN(N_3)$ was found to lead through several intermediates to $PPN[Ru_4(NCO)(CO)_{13}]$. The structure of this product is proposed to be analogous to $[Ru_4Cl(CO)_{13}]^-$ with the μ-NCO replacing the chloride. Spectroscopic characterization of the intermediates suggests that their formulations are $[Ru_3(NCO)(CO)_{11}]^-$ and $[Ru_3(NCO)(CO)_{10}]^-$. Protonation of the initial reaction solution containing these trimers allows the isolation of $HRu_3(NCO)(CO)_{10}$ in low yield. The tetranuclear cluster reacts with CO at room temperature to give $[Ru_3(NCO)(CO)_{11}]^-$, and it reacts with H_2 under the same conditions to give $[H_2Ru_4(NCO)(CO)_{12}]^-$. This anion reacts with CF_3SO_3H to give $H_3Ru_4(NCO)(CO)_{12}$, which was characterized by a single-crystal X-ray crystallographic study [$P2_1/n$ space group; a = 9.836 (2), b = 22.063 (5), c = 10.056 (2) Å; β = 97.93 (1)°; V = 2161 (1) Å^3; Z = 4; final R = 0.024; final R_w = 0.028]. The structure contains a butterfly arrangement of ruthenium tricarbonyl groups with the isocyanate bridging the open edge. The hydrogen atoms were located and refined.

Introduction

The reaction of azide ion with mononuclear metal carbonyls generates, in several examples, a coordinated isocyanate (eq 1) via a rearrangement analogous to the Curtis reaction of acyl

$$LnM{-}CO + N_3^- \rightarrow [LnM{-}NCO]^- + N_2 \quad (1)$$

$$R{-}C(=O){-}Cl + N_3^- \rightarrow R{-}NCO + N_2 + Cl^- \quad (2)$$

halides with azides (eq 2).[1] The extension of this reaction (eq 1) to polynuclear metal carbonyls has thus far not been reported. Further, there are very few examples of cluster coordinated isocyanate, a ligand that can bind to metals in several different modes.[2] Of the two reported examples, one has been structurally characterized and was prepared by the unique reaction of $Ru_3(CO)_{12}$ with $C_6H_{10}N_2$ (eq 3), producing

$$Ru_3(CO)_{12} + C_6H_{10}N_2 \rightarrow \quad (3)$$

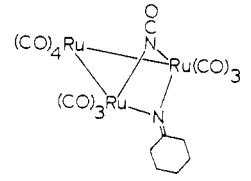

1

1, which contains a doubly bridging NCO ligand.[3] Another example, $HOs_3(NCO)(CO)_{10}$ (**2**), was recently reported[4] to

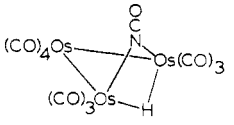

2

result from the reaction of HNCO with $Os_3(CO)_{10}(CH_3CN)_2$ in 87% yield. Of particular interest was the observation that the μ-NCO group in **2** was susceptible to nucleophilic attack by hydrazine to give the urea derivative **3**.

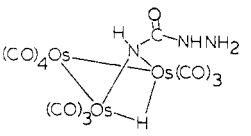

3

Our interest in isocyanate and azide was stimulated by the recent studies of nitrido clusters.[5] In most cases these nitrido clusters are formed by the cleavage of an NO bond of a coordinated nitrosyl ligand or nitrosonium ion. In principle, a nitrogen atom could also be introduced into a cluster with use of NCO^- or N_3^-. If a coordinated isocyanate was isolated, hydrolysis could be used to effect decarboxylation.[6] We present here our studies on the reaction of N_3^- with $Ru_3(CO)_{12}$ and the subsequent reactions of the isocyanato clusters.

Experimental Section

$PPN(Cl)$[7] (PPN = bis(triphenylphosphine)nitrogen(1+)), $PPN(N_3)$,[8] $Ru_3(CO)_{12}$,[9] $PPN[Ru_4Cl(CO)_{13}]$,[10] and $Re(NCO)(CO)_5$[18] were prepared according to published procedures. $Me_3NO{\cdot}2H_2O$ was purchased from Aldrich and used as received. Tetrahydrofuran (THF), diglyme, and diethyl ether were dried by distillation from sodium-benzophenone ketyl under N_2. Methanol was dried by distillation from $Mg(OCH_3)_2$. Hexane and methylene chloride were distilled from P_2O_5 prior to use. All gases were purchased from Matheson and used without further purification. Chromatography was conducted on silica gel, with hexane as the eluent. A summary of the spectroscopic data for each of the compounds appears in Table I.

Preparation of $PPN[Ru_4(NCO)(CO)_{13}]$. $PPN(N_3)$ (195 mg, 0.336 mmol) and $Ru_3(CO)_{12}$ (217 mg, 0.340 mmol) were placed together in a Schlenk tube, and 20 mL of THF was added by syringe. Vigorous evolution of gas accompanied a color change from orange to red. This solution was stirred until all $PPN(N_3)$ was consumed ($\sim^1/_2$ h). After

(1) (a) Beck, W.; Smedal, H. S. *Angew. Chem., Int. Ed. Engl.* **1966**, *5*, 253. (b) Beck, W.; Werner, H.; Engelmann, H.; Smedal, H. S. *Chem. Ber.* **1968**, *101*, 2143. (c) Angelici, R. J.; Busetto, L. *J. Am. Chem. Soc.* **1969**, *91*, 3197. (d) Werner, H.; Beck, W.; Engelmann, H. *Inorg. Chim. Acta* **1969**, *3*, 331. (e) Kruse, A. E.; Angelici, R. J. *J. Organomet. Chem.* **1970**, *24*, 231. (f) Angelici, R. J.; Kruse, A. E. *Ibid.* **1970**, *22*, 461. (g) Angelici, R. J.; Faber, G. C. *Inorg. Chem.* **1971**, *10*, 514.
(2) Norbury, A. H. *Adv. Inorg. Chem. Radiochem.* **1975**, *17*, 231.
(3) Kisch, H.; Riemer, A.; Mastropasqua, P.; Kruger, C. *J. Organomet. Chem.* **1978**, *148*, C40-C42.
(4) Deeming, A. J.; Ghatak, I.; Owen, D. W.; Peters, R. *J. Chem. Soc., Chem. Commun.* **1982**, 392-393.
(5) (a) Martinengo, S.; Ciani, G.; Sironi, A.; Heaton, B. T.; Mason, J. *J. Am. Chem. Soc.* **1979**, *101*, 7095-7097. (b) Tachikawa, M.; Stein, J.; Muetterties, E. L.; Teller, R. G.; Beno, M. A.; Gebert, E.; Williams, J. M. *Ibid.* **1980**, *102*, 6648-6649. (c) Fjare, D.; Gladfelter, W. L. *Ibid.* **1981**, *103*, 1572-1574. (d) Feasey, N.; Knox, S.; Orpen, A. *J. Chem. Soc., Chem. Commun.* **1982**, 75. (e) Martinengo, S.; Ciani, G.; Sironi, A. *J. Am. Chem. Soc.* **1982**, *104*, 328.
(6) (a) Ford, P. C. *Inorg. Chem.* **1971**, *10*, 2153. (b) Werner, K. V.; Beck, W. *Chem. Ber.* **1972**, *105*, 3947.
(7) Ruff, J. K.; Schlentz, W. J. *Inorg. Synth.* **1974**, *15*, 85-87.
(8) Martinsen, A.; Songstad, J. *Acta Chem. Scand., Ser. A* **1977**, *A31*, 645-650.
(9) Mantovani, A.; Cenini, S. *Inorg. Synth.* **1975**, *16*, 47-48.
(10) Steinmetz, G. R.; Harley, A. D.; Geoffroy, G. L. *Inorg. Chem.* **1980**, *19*, 2985-2989.

0020-1669/83/1322-1774$01.50/0

Table I. Spectroscopic Data

cluster	color	δ ($CDCl_3$)	ν_{NCO}, cm^{-1}	ν_{CO}, cm^{-1}
$PPN[Ru_4(NCO)(CO)_{13}]$	red/purple		2189 s (THF)	2061 vw, 2028 s, 2004 vs, 1970 m, br, 1945 sh, 1842 w (THF)
$PPN[H_2Ru_4(NCO)(CO)_{12}]$	red	−13.93	2188 s (THF)	2070 w, 2040 s, 2020 s, 2001 s, 1965 m (THF)
$H_3Ru_4(NCO)(CO)_{12}$	orange	−16.09	2193 s (hexane)	2109 w, 2086 s, 2070 s, 2034 m, 2027 m, 2020 m (hexane)
$HRu_3(NCO)(CO)_{10}$	red	−13.19	2213 s (hexane)	2110 w, 2077 s, 2068 s, 2029 vs, 2002 w (hexane)
$PPN[Ru_3(NCO)(CO)_{11}]$	orange		2230 m, br (THF)	2098 vw, 2060 m, 2028 vs, 2011 s, 1963 m, 1830 m (THF)
$PPN[Ru_3(NCO)(CO)_{10}]$	red		2209 s (THF)	2068 m, 2025 s, 1985 s, br, 1910 m, 1779 m (THF)

the THF was removed under vacuum, the product was extracted with 40 mL of Et_2O, filtered, and layered with hexane. After 2 days this gave 239 mg of dark red, slightly air-sensitive crystals, 70% yield based on Ru. Anal. Calcd for $PPN[Ru_4(NCO)(CO)_{13}]$: C, 44.52; H, 2.24; N, 2.08. Found: C, 44.58; H, 2.34; N, 2.04.

Preparation of $PPN[H_2Ru_4(NCO)(CO)_{12}]$. A. $PPN[Ru_4(NCO)(CO)_{13}]$ (37.5 mg, 0.028 mmol) was dissolved in 10 mL of THF and placed under an H_2 atmosphere. Within 30 min the color had turned from deep red-purple to light red. The infrared spectrum was consistent with the formation of $[H_2Ru_4(NCO)(CO)_{12}]^-$.

B. $H_2Ru_4(CO)_{13}$ (15 mg. 0.020 mmol) was dissolved in 10 mL of THF and added by cannula to another Schlenk tube containing $PPN(N_3)$ (18 mg, 0.031 mmol). An immediate color change was observed, and the IR spectrum indicated formation of the same cluster as in A. The solution of $[H_2Ru_4(NCO)(CO)_{12}]^-$ was filtered from unreacted $PPN(N_3)$ to give a pure solution of $PPN[H_2Ru_4(NCO)(CO)_{12}]$.

Preparation of $H_3Ru_4(NCO)(CO)_{12}$. $PPN[Ru_4(NCO)(CO)_{13}]$ (354 mg, 0.263 mmol) was dissolved in 20 mL of CH_2Cl_2 and placed under an H_2 atmosphere for 45 min. At this time 30 μL of CF_3SO_3H (0.30 mmol) was added by syringe. The CH_2Cl_2 was evaporated, and the neutral products were extracted into hexane. These were chromatographed on silica gel and eluted in the following order. The first band was yellow and contained $H_4Ru_4(CO)_{12}$. The second was red and contained $H_2Ru_4(CO)_{13}$. The third band was orange and gave $H_3Ru_4(NCO)(CO)_{12}$ in 20% yield (38 mg). Anal. Calcd for $H_3Ru_4(NCO)(CO)_{12}$: C, 19.88; H, 0.38; N, 1.78. Found: C, 20.11; H, 0.43; N, 1.74.

Preparation of $HRu_3(NCO)(CO)_{10}$. $PPN(N_3)$ (209 mg, 0.360 mmol) and $Ru_3(CO)_{12}$ (230 mg, 0.360 mmol) were placed together in a Schlenk tube, and 40 mL of THF was added by syringe. The solution was stirred until all $PPN(N_3)$ was consumed and then acidified with 40 μL of CF_3SO_3H (0.40 mmol). Evaporation of the THF and extraction of the neutral products in hexane gave several products, which were separated by column chromatography. The first band to elute was $Ru_3(CO)_{12}$, the major product. The next band was red and contained $H_2Ru_4(CO)_{13}$. The third band was also red and was identified as $HRu_3(NCO)(CO)_{10}$, isolated in 7% yield (15 mg). Anal. Calcd for $HRu_3(NCO)(CO)_{10}$: C, 21.09; H, 0.16; N, 2.24. Found: C, 21.29; H, 0.18; N, 2.20.

Protonation of $PPN[Ru_4(NCO)(CO)_{13}]$. $PPN[Ru_4(NCO)(CO)_{13}]$ (102 mg, 0.076 mmol) was placed in a Schlenk tube and 10 mL of CH_2Cl_2 was distilled under reduced pressure. To this solution was added 8 μL of CF_3SO_3H (0.08 mmol). Evaporation of the CH_2Cl_2 and extraction of the residue with hexane gave $Ru_3(CO)_{12}$ as the only hexane-soluble product.

Collection and Reduction of the X-ray Data. Orange crystals of $H_3Ru_4(NCO)(CO)_{12}$ were grown by slow cooling of a saturated hexane solution, one of which was mounted on a glass fiber. The crystal was found to be monoclinic by the Enraf-Nonius CAD4-SDP peak search, centering, and indexing programs and by a Delauney reduction calculation.[11] A summary of the crystal data is presented in Table II. Background counts were measured at both ends of the scan range with the use of a ω–2θ scan, equal at each side to one-fourth of the scan range of the peak. In this manner, the total duration of measuring background is equal to half of the time required for the peak scan. The three check reflections showed no change in intensity during data collection. A total of 4779 unique reflections were measured, of which

Table II

Crystal Parameters	
cryst syst: monoclinic	$V = 2161$ (1) Å^3
space group: $P2_1/n$	$Z = 4$
$a = 9.836$ (2) Å	calcd density: 2.414 g/cm^3
$b = 22.062$ (5) Å	temp: 22 °C
$c = 10.056$ (2) Å	abs coeff: 27.38 cm^{-1}
$\beta = 97.93$ (1)°	formula: $C_{13}H_3NO_{13}Ru_4$

Measurement of Intensity Data

diffractometer: Enraf-Nonius CAD4
radiation: Mo Kα (λ = 0.710 69 Å)
monochromator: graphite cryst
scan speed: variable between 0.6 and 20°/min
scan range: $0° \leq 2\theta \leq 52°$
reflctns measd: $+h, +k, \pm l$
check reflctns: {−4,0,4}, {2,10,−1}, {4,0,4}; measd approx every 90 reflctns
reflctns collected: 4779 unique reflctns; 3094 with $I > 2.0\sigma(I)$
$p = 0.04$
$R = 0.024$
$R_w = 0.028$

3094 had $I > 2.0\sigma(I)$ and were used in the structural determination.[12] The data were corrected for Lorentz, polarization, and background effects and for absorption. The space group $P2_1/n$ was chosen on the basis of the systematic absences.

Solution and Refinement of the Structure. The structure was solved by conventional heavy-atom techniques. The positions of the four ruthenium atoms were determined from a Patterson synthesis. Subsequent difference Fourier calculations revealed the positions of the non-hydrogen atoms.[13] After these atoms were refined with anisotropic thermal parameters, a difference map revealed the positions of the three bridging hydrogens as the three largest peaks. The positions and thermal parameters of all atoms were refined, the hydrogen atoms with isotropic thermal parameters only, in the subsequent least-squares cycles. The values of the atomic scattering factors used in the calculations were taken from the usual tabulation,[14] and the effects of anomalous dispersion were included for all non-hydrogen atoms.[15]

Results and Discussion

The reaction of azide with $Ru_3(CO)_{12}$ is complex and is characterized by several stages. In the following discussion we will present the results of experiments designed to elucidate the structures of the intermediate clusters and the nature of the interconversions. Since several of these compounds could

(11) All calculations were carried out on PDP 8A and 11/34 computers using the Enraf-Nonius CAD 4-SDP programs. This crystallographic computing package is described in: Frenz, B. A. In "Computing in Crystallography"; Schenk, H., Olthof-Hzekamp, R., van Koningsveld, H., Bassi, G. C., Eds.; Delft University Press: Delft, Holland, 1978; pp 64–71. See also: "CAD 4 and SDP Users Manual"; Enraf-Nonius: Delft, Holland, 1978.

(12) The intensity data were processed as described: "CAD 4 and SDP Users Manual"; Enraf-Nonius: Delft, Holland, 1978. The net intensity $I = (K/NPI)(C - 2B)$, where $K = 20.1166_x$ (attenuator factor), NPI = ratio of fastest possible scan rate to scan rate for the measurement, C = total count, and B = total background count. The standard deviation in the net intensity is given by $\sigma^2(I) = (K/NPI)^2[C + 4B + (pI)^2]$, where p is a factor used to downweight intense reflections. The observed structure factor amplitude F_o is given by $F_o = (I/Lp)^{1/2}$, where Lp = Lorentz and polarization factors. The $\sigma(I)$'s were converted to the estimated errors in the relative structure factors $\sigma(F_o)$ by $\sigma(F_o) = {}^1/_2(\sigma(I)/I)F_o$.

(13) The function minimized was $\sum w(|F_o| - |F_c|)^2$, where $w = 1/\sigma^2(F_o)$. The unweighted and weighted residuals are defined as $R = (\sum||F_o| - |F_c||)/\sum|F_o|$ and $R_w = [(\sum w(|F_o| - |F_c|))^2/(\sum w|F_o|)^2]^{1/2}$. The error in an observation of unit weight is $[\sum w(|F_o| - |F_c|)^2/(NO - NV)]^{1/2}$, where NO and NV are the numbers of observations and variables, respectively.

(14) Cromer, D. T.; Waber, J. T. "International Tables for X-ray Crystallography"; Kynoch Press: Birmingham, England, 1974; Vol. IV, Table 2.2.A.

(15) Cromer, D. T.; Ibers, J. A. "International Tables for X-ray Crystallography"; Kynoch Press: Birmingham, England, 1974; Vol. IV, Table 2.3.1.

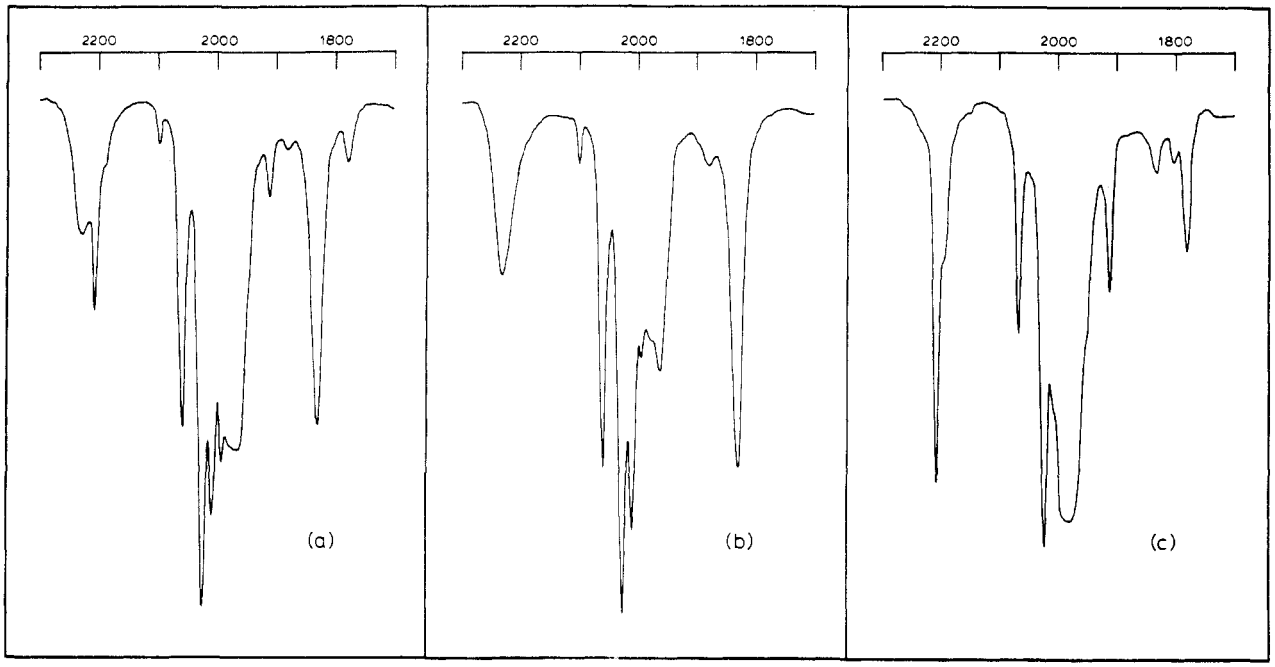

Figure 1. Carbonyl and isocyanato region of the infrared spectrum in THF resulting from (a) initial solution of $Ru_3(CO)_{12}$ and $PPN(N_3)$, (b) solution from (a) plus CO (1 atm), and (c) solution from (a) plus Me_3NO.

not be isolated in crystalline form, we have had to rely heavily on infrared spectroscopy and the use of known reactions to characterize the intermediates.

Overview of the Reaction. When $Ru_3(CO)_{12}$ is mixed with $PPN(N_3)$ in THF solution, vigorous bubbling occurs as the color changes from orange to red. Details of the infrared spectroscopic changes will be presented below. After all of the $PPN(N_3)$ is consumed (30 min), the solvent is removed in vacuo. Extraction of the dark red residue with ether and slow diffusion of hexane into the solution allows the isolation of $PPN[Ru_4(NCO)(CO)_{13}]$ in 70% yield. This material has been well characterized, but it is clear from observation of the initial reaction solution that several intermediates precede the formation of $[Ru_4(NCO)(CO)_{13}]^-$. By varying the conditions, we have been able to obtain solutions containing two of these intermediates in >90% purity. This has allowed us to monitor their interconversions as well as propose reasonable structures for them.

Stage 1: Formation of $[Ru_3(NCO)(CO)_{11}]^-$. Many studies of the reaction of a metal carbonyl with N_3^- have shown eq 1 to be quite general.[1] If this primary reaction occurs with $Ru_3(CO)_{12}$ (eq 4), the anion $[Ru_3(NCO)(CO)_{11}]^-$ should be

$$Ru_3(CO)_{12} + N_3^- \rightarrow [Ru_3(NCO)(CO)_{11}]^- + N_2 \quad (4)$$

obtained. Figure 1a shows that two species containing an isocyanate ligand (based on the number of absorbances in the ν_{NCO} region) are formed upon mixing N_3^- with $Ru_3(CO)_{12}$, neither of which is the compound, $[Ru_4(NCO)(CO)_{13}]^-$, that is ultimately isolated from the reaction. Figure 1b shows the result of placing this solution under a CO atmosphere. The ν_{NCO} band at 2209 cm^{-1} completely disappears, and a clear spectrum of what we propose to be $[Ru_3(NCO)(CO)_{11}]^-$ is obtained rapidly. This identical spectrum is also obtained from mixing $Ru_3(CO)_{12}$ and $PPN(N_3)$ in THF under a CO atmosphere. The rate of product formation does not appear to be affected by the presence of CO, suggesting that loss of a carbonyl is not involved in the rate-determining step.

The $\nu_{s(NCO)}$ region of the infrared spectrum is particularly helpful in identifying the three different anions observed, as well as being a valuable structural tool. The two absorbances initially observed appear at 2230 and 2209 cm^{-1}. Further, these absorbances differ substantially in appearance. The higher energy peak is broad and only of medium intensity compared to a strong sharp absorbance at lower energy. As seen in Table I, of the six new isocyanato clusters prepared, all except $[Ru_3(NCO)(CO)_{11}]^-$ have the strong, sharp absorbance that we attribute to a bridging isocyanate group. Figure 2 shows a spectroscopic comparison of $[Ru_3(NCO)$-

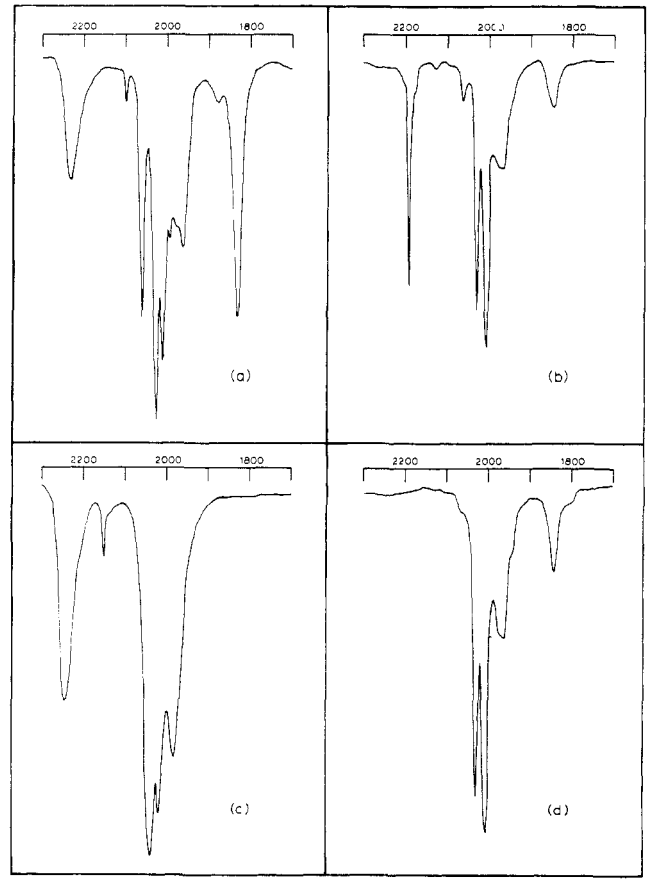

Figure 2. Comparison of the carbonyl and isocyanato region of the infrared spectrum in THF of (a) $PPN[Ru_3(NCO)(CO)_{11}]$, (b) $PPN[Ru_4(NCO)(CO)_{13}]$, (c) $Re(NCO)(CO)_5$, and (d) $PPN[Ru_4Cl(CO)_{13}]$.

$(CO)_{11}]^-$, $[Ru_4(NCO)(CO)_{13}]^-$, and $Re(NCO)(CO)_5$,[18] which clearly illustrates the different ν_{NCO} peak shapes for these carbonyl isocyanato complexes. Previous studies of isocyanato complexes in every case prove this observation to be general.[2] Although few X-ray crystallographic studies have been conducted on metal isocyanato complexes, those terminal isocyanato ligands studied have been found to form a linear MNCO linkage as shown in **4**, while the η^1 bridging NCO

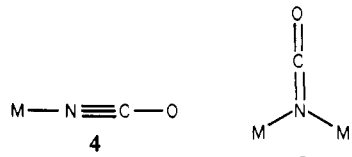

4 **5**

ligand binds as shown in **5**. Since $\nu_{s(NCO)}$ is comprised principally of the C–N stretch, it is clear why the energy of ν_s is lowered in going from a linear, terminal NCO to a bridging ligand.

Returning now to the structure of $[Ru_3(NCO)(CO)_{11}]^-$, we note that there is a strong bridging CO stretch at 1830 cm^{-1}. With the restrictions of having a terminal isocyanate and a bridging CO, the only reasonable structure, **6**, is one based

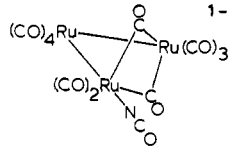

6

on the structure of $Fe_3(CO)_{12}$.[16] Although no data is available to allow assignment of the position of the NCO, we have chosen to place it as shown for two reasons. First, in solution the clusters $Fe_3(CO)_{11}(L)$, where L = $PPhMe_2$, $P(OEt)_3$, and $P(OPh)_3$, are substituted in this position.[17] Second, the bridging carbonyls are bound to the Ru containing the excess negative charge. That only one bridging CO resonance is observed for this structure is explained by the trans orientation of the bridging ligands. As the two CO vectors become collinear, the dipole moment change of the symmetric stretch greatly decreases, thus affecting the intensity of this transition. A close inspection of Figure 1 does in fact show a very weak absorbance at 1879 cm^{-1} associated with $[Ru_3(NCO)(CO)_{11}]^-$ that could be assigned to the symmetric stretch of the bridging carbonyls.

Stage 2: Formation of $[Ru_3(NCO)(CO)_{10}]^-$. The second compound observed in the reaction mixture of N_3^- and $Ru_3(CO)_{12}$ is related to $[Ru_3(NCO)(CO)_{11}]^-$ by conversion of the terminal NCO to a bridging position and loss of a CO. Figure 1a shows the infrared spectrum of the original mixture. When Me_3NO is added to this solution, a clean conversion occurs to generate the spectrum shown in Figure 1c (eq 5). All of

$$[Ru_3(NCO)(CO)_{11}]^- + Me_3NO \rightarrow CO_2 + Me_3N + [Ru_3(NCO)(CO)_{10}]^- \quad (5)$$

the NCO absorbance at 2230 cm^{-1} has disappeared, and the sharp absorbance at 2209 cm^{-1} has increased in intensity. This same conversion occurs thermally given enough time, but this reaction is complicated by subsequent steps discussed below. When the solution containing only $[Ru_3(NCO)(CO)_{10}]^-$ is placed under a CO atmosphere, $[Ru_3(NCO)(CO)_{11}]^-$ is quantitatively and rapidly regenerated.

Protonating a solution containing a mixture of $[Ru_3(NCO)(CO)_{10}]^-$ and $[Ru_3(NCO)(CO)_{11}]^-$ with CF_3SO_3H gives $Ru_3(CO)_{12}$ as the major isolated species. A small amount of $HRu_3(NCO)(CO)_{10}$ does form and can be isolated chromatographically. The ν_{NCO} band appears at 2213 cm^{-1}, only 4 cm^{-1} higher than in $[Ru_3(NCO)(CO)_{10}]^-$. The carbonyl region of the infrared spectrum and the ^1H NMR spectrum of $HRu_3(NCO)(CO)_{10}$ indicate that it is clearly isostructural (**7**) to the many other examples of $HRu_3(X)(CO)_{10}$ clusters,[18] as well as the corresponding osmium analogue $HOs_3(NCO)(CO)_{10}$.[4]

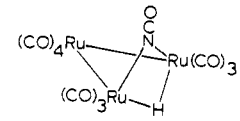

7

The structure of $[Ru_3(NCO)(CO)_{10}]^-$ is not so easily assigned. That it has a μ-NCO group in a position similar to that for its protonated form is evidenced by the similarity of their ν_{NCO} absorbances. Yet the most obvious structure, analogous to that proposed for $[Ru_3(CO)_{10}(NO)]^-$[19] (**8**),

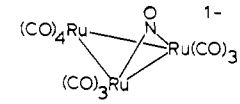

8

cannot be correct, since a bridging carbonyl stretch is observed at 1779 cm^{-1} in $[Ru_3(NCO)(CO)_{10}]^-$. Kaesz and co-workers have recently reported[20] the synthesis of $[Ru_3(\mu\text{-}O{=}C(NMe_2))(CO)_{10}]^-$, which has two bridging CO absorbances at 1813 and 1796 cm^{-1}. In analogy to the case for $Ru_3(N_2C_4H_4)(CO)_{10}$,[21] they proposed that it has the structure shown in **9** with three bridging carbonyls. We believe it is highly

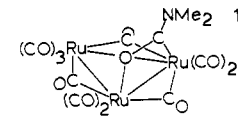

9

unlikely that $[Ru_3(NCO)(CO)_{10}]^-$ adopts this structure for two reasons. The stretching frequency of NCO would undoubtedly be strongly shifted if the ligand was coordinated in any *multihapto* fashion. Second, it is unlikely that a structure such as **9** would exist with a simple η^1 ligand. We propose that the structure of $[Ru_3(NCO)(CO)_{10}]^-$ be based on that recently found[22] for $[Fe_3(CO)_{11}]^{2-}$ (**10**), in which the μ-NCO

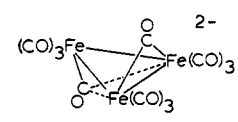

10

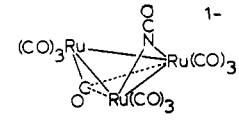

11

ligand replaces μ-CO (**11**). Such a proposal can account for the spectral data mentioned above and is, in fact, quite similar to the structure of $[Ru_3(CO)_{10}(NO)]^-$ (**8**). Simple electron counting gives a clue as to why $[Ru_3(NCO)(CO)_{10}]^-$ contains a bridging CO. In $[Ru_3(CO)_{10}(NO)]^-$, the negative charge is equally distributed on the two metals bridged by the NO ligand. In $[Ru_3(NCO)(CO)_{10}]^-$, a similar structure would place the negative charge on the two metals bridged by μ-

(16) (a) Wei, C. H.; Dahl, L. F. *J. Am. Chem. Soc.* **1966**, *88*, 1821. (b) Cotton, F. A.; Troup, J. M. *Ibid.* **1974**, *96*, 4155.
(17) Benfield, R. E.; Gavens, P. D.; Johnson, B. F. G.; Mays, M. J.; Aime, S.; Milone, L.; Osella, D. *J. Chem. Soc., Dalton Trans.* **1981**, 1535.
(18) Boag, N. M.; Kampe, C. E.; Lin, Y. C.; Kaesz, H. D. *Inorg. Chem.* **1982**, *103*, 4981.
(19) Stevens, R. E.; Yanta, T. J.; Gladfelter, W. L. *J. Am. Chem. Soc.* **1981**, *103*, 4981.
(20) Mayr, A.; Lin, Y. C.; Boag, N. M.; Kaesz, H. D. *Inorg. Chem.* **1982**, *21*, 1704.
(21) Cotton, F. A.; Hanson, B. E.; Jamerson, J. D. *J. Am. Chem. Soc.* **1977**, *99*, 6588.
(22) Lo, F.; Longoni, G.; Chini, P.; Lower, L.; Dahl, L. F. *J. Am. Chem. Soc.* **1980**, *102*, 7691.

NCO, which is not an effective π-accepting ligand. Formation of a semi-triply bridging carbonyl allows the charge to be delocalized over all three metals. Considering NO is the most effective π-accepting ligand, the need for $[Ru_3(CO)_{10}(NO)]^-$ to adopt a structure such as **11** is greatly reduced.

Stage 3: Conversion to $[Ru_4(NCO)(CO)_{13}]^-$. There are no spectroscopically observable intermediates between $[Ru_3(NCO)(CO)_{10}]^-$ and the product that is ultimately isolated as crystalline material, $[Ru_4(NCO)(CO)_{13}]^-$. This conversion is very slow (several days) if the solution of $[Ru_3(NCO)(CO)_{11}]^-$ and $[Ru_3(NCO)(CO)_{10}]^-$ is stirred at room temperature. If the reaction is refluxed, other currently uncharacterized products also form. This is not simply pyrolysis of $[Ru_4(NCO)(CO)_{13}]^-$ itself since it is stable in refluxing THF for at least 2 h. We discovered that the simplest method to form $[Ru_4(NCO)(CO)_{13}]^-$ was to remove the solvent under vacuum and extract the residue with ether. Figure 3 shows a series of infrared spectra from successive concentrations under vacuum followed by dissolution in fresh THF. The spectra clearly show the sequential formation and disappearance of $[Ru_3(NCO)(CO)_{11}]^-$ and $[Ru_3(NCO)(CO)_{10}]^-$. As absorbances due to the latter cluster disappear (most notably the 2209-cm^{-1} peak), the formation of $[Ru_4(NCO)(CO)_{13}]^-$ occurs. It seems that concentrating the solutions under vacuum has the dual effect of removing CO as it is formed (the reaction reverts under CO as discussed below) and increasing the rate of the reaction. Unfortunately, we do not know the overall stoichiometry of this conversion; therefore, further speculation regarding the mechanism is unwarranted.

The structure of $[Ru_4(NCO)(CO)_{13}]^-$ (**12**) is the same as

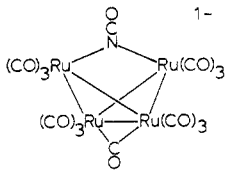

12

that for $[Ru_4Cl(CO)_{13}]^-$,[10] with μ-NCO replacing μ-Cl. This proposal is based on the nearly identical infrared spectra of the two clusters (Figure 2) with the exception of the isocyanate stretching frequency at 2189 cm^{-1}, which is lowered in energy relative to that for $[Ru_3(NCO)(CO)_{10}]^-$. When a solution of $[Ru_4(NCO)(CO)_{13}]^-$ at room temperature is reacted with CO (1 atm), conversion to $[Ru_3(NCO)(CO)_{11}]^-$ and $Ru_3(CO)_{12}$ occurs in 30 min.

Formation and Protonation of $[H_2Ru_4(NCO)(CO)_{12}]^-$. Further characterization of $[Ru_4(NCO)(CO)_{13}]^-$ showed that it reacts with hydrogen under surprisingly mild conditions. When a THF solution of $[Ru_4(NCO)(CO)_{13}]^-$ was stirred at room temperature for 30 min under H_2 (1 atm), the color changed to light red (eq 6). The ν_{NCO} band remained virtually

$$[Ru_4(NCO)(CO)_{13}]^- + H_2 \rightleftharpoons [H_2Ru_4(NCO)(CO)_{12}]^- + CO \quad (6)$$

unchanged at 2188 cm^{-1}, but the bridging carbonyl absorbance had completely disappeared. The ^1H NMR spectrum in $CDCl_3$ exhibited a single resonance at −13.93 ppm. Attempts at crystallization were foiled by the reversion of $[H_2Ru_4(NCO)(CO)_{12}]^-$ to $[Ru_4(NCO)(CO)_{13}]^-$ and insoluble material. The complex $[H_2Ru_4(NCO)(CO)_{12}]^-$ is also not stable under H_2, forming $[H_3Ru_4(CO)_{12}]^-$ cleanly in ~1 day.

An independent route to $[H_2Ru_4(NCO)(CO)_{12}]^-$ was found by reacting $H_2Ru_4(CO)_{13}$ with $PPN(N_3)$ (eq 7), which further

$$H_2Ru_4(CO)_{13} + N_3^- \rightarrow N_2 + [H_2Ru_4(NCO)(CO)_{12}]^- \quad (7)$$

illustrates the specificity of the reaction of azide with metal carbonyl clusters. The possible structures of $[H_2Ru_4(NCO)(CO)_{12}]^-$ are shown in **13** and **14** and differ only in the position of one of the hydrogen atoms. It is not unlikely that both isomers exist and are rapidly interconverting.

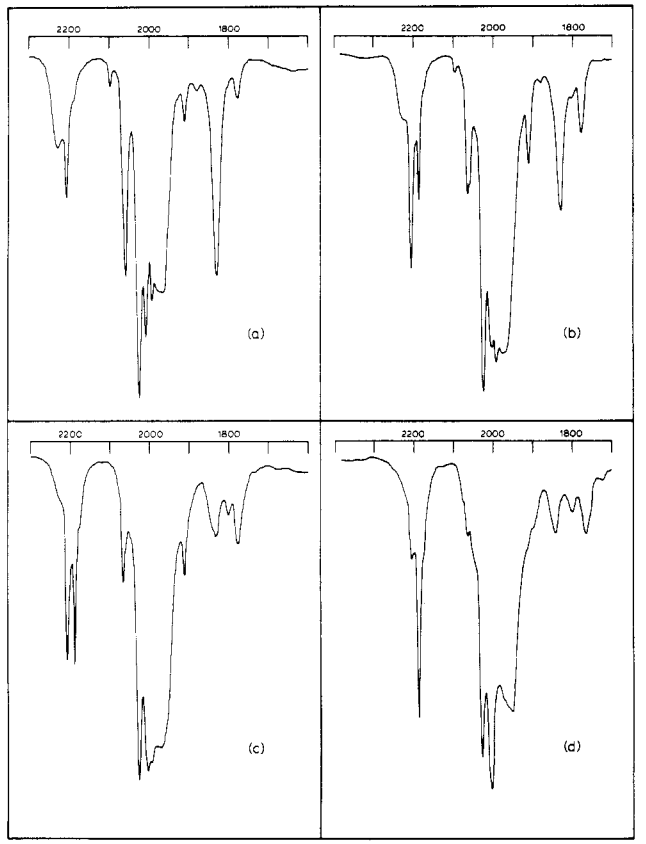

Figure 3. Carbonyl and isocyanato region of the infrared spectrum in THF solution of (a) a mixture of $Ru_3(CO)_{12}$ and $PPN(N_3)$, (b) the mixture after ~12 of stirring under N_2, (c) the mixture after evaporation and redissolution in THF, and (d) the mixture after five cycles of evaporation and redissolution in THF.

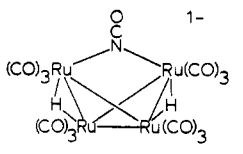

13

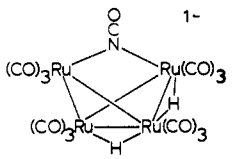

14

Protonation of a CH_2Cl_2 solution of $[H_2Ru_4(NCO)(CO)_{12}]^-$ with CF_3SO_3H followed by evaporation, extraction of the residue into hexane, and chromatography results in the isolation of $H_4Ru_4(CO)_{12}$, $H_2Ru_4(CO)_{13}$, and $H_3Ru_4(NCO)(CO)_{12}$. The latter is obtained in 20% yield based upon the initial amount of $[Ru_4(NCO)(CO)_{13}]^-$ reacted with H_2. The red crystalline material was volatile enough to obtain a mass spectrum, which did not exhibit a parent ion. The highest peak observed was for the fragment $[H_nRu_4(CO)_{12}]^+$, indicating facile loss of the NCO group. The ν_{NCO} band (2193 cm^{-1}) increases by 4 cm^{-1} relative to that of $[H_2Ru_4(NCO)(CO)_{12}]^-$. It is noteworthy that this magnitude increase is identical with that observed when converting $[Ru_3(NCO)(CO)_{10}]^-$ into $HRu_3(NCO)(CO)_{10}$. The ^1H NMR spectral study (Figure 4) indicates that the unique bond in **13** or **14** is protonated, giving a structure of C_2 symmetry (**15**). The hydrogens

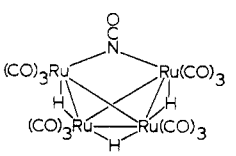

15

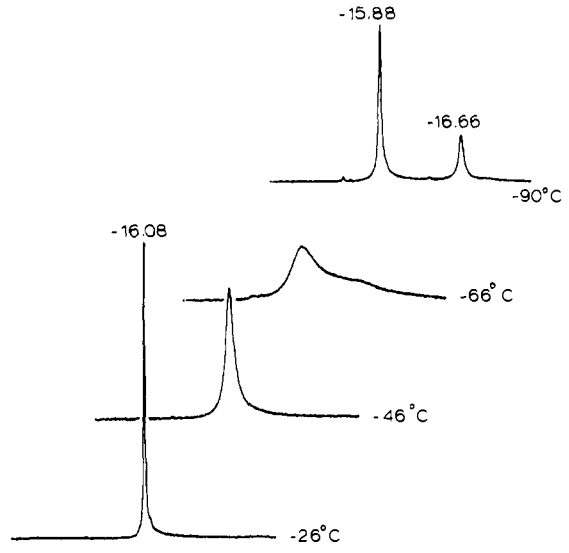

Figure 4. Dynamic ^1H NMR spectra of $H_3Ru_4(NCO)(CO)_{12}$ in CD_2Cl_2.

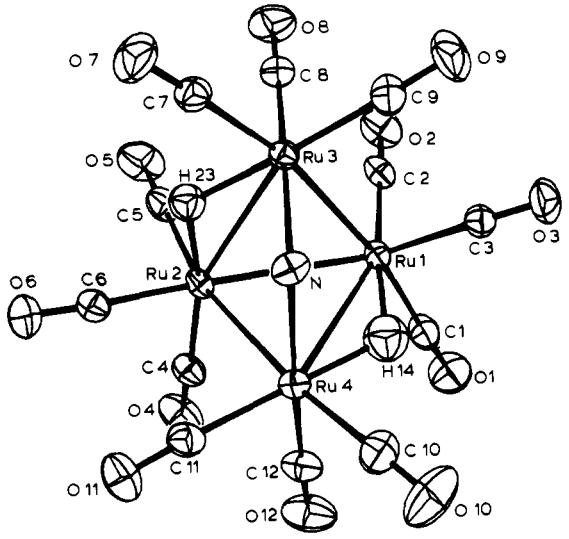

Figure 5. View of $H_3Ru_4(NCO)(CO)_{12}$ down the pseudo-C_2 axis showing the atom labels. Atoms C and O of the isocyanate and H(12) are not shown.

Table III. Bond Distances (Å)

Ru(1)-Ru(2)	2.949 (1)	Ru(2)-C(6)	1.890 (6)
Ru(1)-Ru(3)	2.823 (1)	Ru(3)-C(7)	1.952 (6)
Ru(1)-Ru(4)	3.009 (1)	Ru(3)-C(8)	1.862 (6)
Ru(2)-Ru(3)	3.021 (1)	Ru(3)-C(9)	1.913 (6)
Ru(2)-Ru(4)	2.825 (1)	Ru(4)-C(10)	1.941 (7)
Ru(1)-H(12)	1.79 (6)	Ru(4)-C(11)	1.910 (6)
Ru(1)-H(14)	1.75 (6)	Ru(4)-C(12)	1.871 (6)
Ru(2)-H(12)	1.83 (6)	C(1)-O(1)	1.111 (6)
Ru(2)-H(23)	1.79 (5)	C(2)-O(2)	1.139 (7)
Ru(3)-H(23)	1.76 (5)	C(3)-O(3)	1.128 (6)
Ru(4)-H(14)	1.71 (6)	C(4)-O(4)	1.119 (6)
Ru(3)-N	2.144 (4)	C(5)-O(5)	1.132 (7)
Ru(4)-N	2.151 (4)	C(6)-O(6)	1.133 (6)
N-C	1.153 (7)	C(7)-O(7)	1.116 (6)
C-O	1.179 (7)	C(8)-O(8)	1.134 (6)
Ru(1)-C(1)	1.955 (6)	C(9)-O(9)	1.132 (6)
Ru(1)-C(2)	1.893 (6)	C(10)-O(10)	1.124 (7)
Ru(1)-C(3)	1.896 (5)	C(11)-O(11)	1.128 (6)
Ru(2)-C(4)	1.922 (6)	C(12)-O(12)	1.132 (6)
Ru(2)-C(5)	1.929 (6)		

interchange positions at low temperature consistent with the idea[23] that structures that have "vacant", equivalent positions

(23) Knox, S. A. R.; Kesz, H. D. *J. Am. Chem. Soc.* **1971**, *93*, 4594.

Table IV. Selected Bond Angles (deg)

Ru(2)-Ru(1)-Ru(3)	63.07 (1)	Ru(1)-Ru(2)-Ru(3)	56.43 (1)
Ru(2)-Ru(1)-Ru(4)	56.59 (1)	Ru(1)-Ru(2)-Ru(4)	62.77 (1)
Ru(3)-Ru(1)-Ru(4)	72.04 (1)	Ru(3)-Ru(2)-Ru(4)	71.84 (1)
Ru(2)-Ru(1)-C(1)	109.4 (2)	Ru(1)-Ru(2)-C(4)	104.5 (2)
Ru(2)-Ru(1)-C(2)	99.9 (2)	Ru(1)-Ru(2)-C(5)	104.8 (2)
Ru(2)-Ru(1)-C(3)	150.0 (2)	Ru(1)-Ru(2)-C(6)	151.5 (2)
Ru(3)-Ru(1)-C(1)	170.3 (2)	Ru(3)-Ru(2)-C(4)	160.0 (2)
Ru(3)-Ru(1)-C(2)	93.6 (2)	Ru(3)-Ru(2)-C(5)	96.6 (2)
Ru(3)-Ru(1)-C(3)	89.5 (2)	Ru(3)-Ru(2)-C(6)	102.6 (2)
Ru(4)-Ru(1)-C(1)	98.8 (2)	Ru(4)-Ru(2)-C(4)	95.0 (2)
Ru(4)-Ru(1)-C(2)	156.0 (2)	Ru(4)-Ru(2)-C(5)	166.2 (2)
Ru(4)-Ru(1)-C(3)	105.4 (2)	Ru(4)-Ru(2)-C(6)	93.8 (2)
C(1)-Ru(1)-C(2)	93.8 (3)	C(4)-Ru(2)-C(5)	94.1 (2)
C(1)-Ru(1)-C(3)	96.3 (2)	C(4)-Ru(2)-C(6)	93.0 (2)
C(2)-Ru(1)-C(3)	93.4 (2)	C(5)-Ru(2)-C(6)	96.1 (3)
H(12)-Ru(1)-C(1)	85.0 (2)	H(12)-Ru(2)-C(4)	81 (2)
H(12)-Ru(1)-C(2)	76.0 (2)	H(12)-Ru(2)-C(5)	81 (2)
H(12)-Ru(1)-C(3)	169 (2)	H(12)-Ru(2)-C(6)	173 (2)
H(14)-Ru(1)-C(1)	85 (2)	H(23)-Ru(2)-C(4)	167 (2)
H(14)-Ru(1)-C(2)	174 (2)	H(23)-Ru(2)-C(5)	87 (2)
H(14)-Ru(1)-C(3)	81 (2)	H(23)-Ru(2)-C(6)	74 (2)
H(12)-Ru(1)-H(14)	110 (3)	H(12)-Ru(2)-H(23)	112 (2)
H(12)-Ru(1)-Ru(2)	36 (2)	H(12)-Ru(2)-Ru(1)	35 (2)
H(12)-Ru(1)-Ru(3)	91 (2)	H(12)-Ru(2)-Ru(3)	84 (2)
H(12)-Ru(1)-Ru(4)	85 (2)	H(12)-Ru(2)-Ru(4)	90 (2)
H(14)-Ru(1)-Ru(2)	85 (2)	H(23)-Ru(2)-Ru(1)	88 (2)
H(14)-Ru(1)-Ru(3)	88 (2)	H(23)-Ru(2)-Ru(3)	31 (2)
H(14)-Ru(1)-Ru(4)	29 (2)	H(23)-Ru(2)-Ru(4)	86 (2)
Ru(1)-Ru(3)-Ru(2)	60.51 (1)	Ru(1)-Ru(4)-Ru(2)	60.64 (1)
Ru(1)-Ru(3)-N	87.0 (1)	Ru(1)-Ru(4)-N	82.2 (1)
Ru(2)-Ru(3)-N	82.8 (1)	Ru(2)-Ru(4)-N	87.6 (1)
Ru(1)-Ru(3)-C(7)	169.4 (2)	Ru(1)-Ru(4)-C(10)	113.3 (2)
Ru(1)-Ru(3)-C(8)	89.7 (2)	Ru(1)-Ru(4)-C(11)	150.6 (2)
Ru(1)-Ru(3)-C(9)	93.4 (2)	Ru(1)-Ru(4)-C(12)	91.9 (2)
Ru(2)-Ru(3)-C(7)	109.6 (2)	Ru(2)-Ru(4)-C(10)	173.7 (2)
Ru(2)-Ru(3)-C(8)	93.0 (2)	Ru(2)-Ru(4)-C(11)	90.3 (2)
Ru(2)-Ru(3)-C(9)	153.7 (2)	Ru(2)-Ru(4)-C(12)	89.1 (2)
N-Ru(3)-C(7)	88.0 (2)	N-Ru(4)-C(10)	89.7 (2)
N-Ru(3)-C(8)	175.5 (2)	N-Ru(4)-C(11)	93.0 (2)
N-Ru(3)-C(9)	93.1 (2)	N-Ru(4)-C(12)	174.2 (2)
C(7)-Ru(3)-C(8)	94.8 (2)	C(10)-Ru(4)-C(11)	95.6 (3)
C(7)-Ru(3)-C(9)	96.2 (2)	C(10)-Ru(4)-C(12)	93.1 (3)
C(8)-Ru(3)-C(9)	90.1 (3)	C(11)-Ru(4)-C(12)	91.9 (3)
H(23)-Ru(3)-C(7)	78 (2)	H(14)-Ru(4)-Ru(1)	30 (2)
H(23)-Ru(3)-C(8)	92 (2)	H(14)-Ru(4)-Ru(2)	90 (2)
H(23)-Ru(3)-C(9)	173 (2)	H(14)-Ru(4)-N	87 (2)
H(23)-Ru(3)-Ru(1)	92 (2)	H(14)-Ru(4)-C(10)	84 (2)
H(23)-Ru(3)-Ru(2)	32 (2)	H(14)-Ru(4)-C(11)	179 (2)
H(23)-Ru(3)-N	85 (2)	H(14)-Ru(4)-C(12)	88 (2)
Ru(3)-N-Ru(4)	106.1 (2)	Ru-C-O (av)	177.6 (9)
Ru(3)-N-C	125.9 (4)	Ru(1)-H(12)-Ru(2)	109 (3)
Ru(4)-N-C	127.8 (4)	Ru(1)-H(14)-Ru(4)	121 (3)
N-C-O	179.3 (7)	Ru(2)-H(23)-Ru(3)	117 (3)

available to accommodate the hydrogens will be fluxional at low temperatures.

Molecular Structure of $H_3Ru_4(NCO)(CO)_{12}$. Figure 5 shows the structure and the atomic labeling scheme of $H_3Ru_4(NCO)(CO)_{12}$. The structure consists of a butterfly arrangement of $Ru(CO)_3$ groups with an N-bound NCO ligand bridging the open edge of the structure. Three hydrogen atoms bridge separate metal–metal bonds such that the overall structure has C_2 symmetry. Tables III and IV present the pertinent bond distance and angle data.

Details of the $H_3Ru_4(NCO)$ geometry are shown in Figure 6. Several points are of interest here. The dihedral angle between the two metal planes (Ru(1)–Ru(2)–Ru(3) and Ru(1)–Ru(2)–Ru(4)) is 85.5°. As recently pointed out by Carty and co-workers,[24] this angle is characteristic of a structure containing 62 electrons. The structure of $H_3Ru_4(NCO)(CO)_{12}$ is similar to that of $H_3Os_4(I)(CO)_{12}$, which was

(24) Carty, A. J.; Maclaughlin, S. A.; Van Wagner, J.; Taylor, N. J. *Organometallics* **1982**, *1*, 1013.

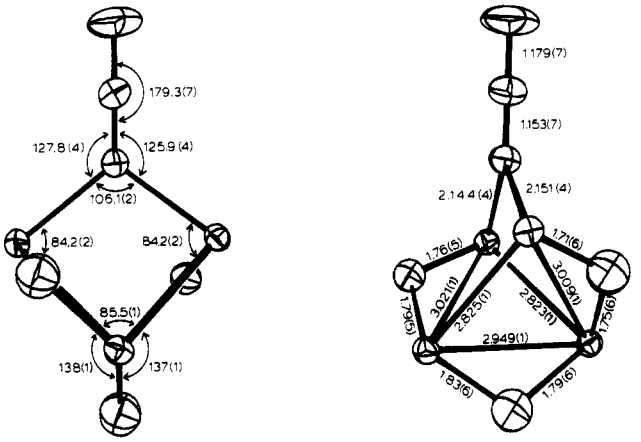

Figure 6. Two views of the $H_3Ru_4(NCO)$ core showing selected distances and angles.

prepared by the reaction of I_2 with $[H_3Os_4(CO)_{12}]^-$.[25] The osmium cluster belongs to the space group $C2/c$ and sits on a crystallographic twofold axis. Although the disposition of carbonyl ligands and the metal–metal bond lengths alluded to the correct hydrogen atom locations, they were not directly observed. The similarities between $H_3Ru_4(NCO)(CO)_{12}$ and $H_3Os_4(I)(CO)_{12}$ certainly confirm the original assignments.

Figure 6 also shows an interesting aspect of the H-atom locations. H(14) and H(23) lie in the triangular plane to which they are bound. The unique hydrogen H(12) almost perfectly bisects the dihedral angle of the butterfly. The coordination geometry around each ruthenium is very close to octahedral, and the six independent trans H–Ru–C angles average 173 (4)°. The two hydrogen environments differ slightly, a result of the shorter Ru(1)–Ru(2) bond distance (2.949 (1) Å) compared to those of Ru(1)–Ru(4) (3.009 (1) Å) and Ru(2)–Ru(3) (3.021 (1) Å).

The isocyanate ligand is assumed to be N bound. Certainly, vibrational spectroscopy indicates this as well as literature precedent.[2] The usual crystallographic test for such an ambiguity would be to switch the two atoms and examine the effect on the temperature factors upon further refinement. In this structure NCO is pointing radially away from the cluster and the two ends already differ substantially in their temperature factors (B_{iso}(N) = 3.4 Å^2; B_{iso}(O) = 10.1 Å^2). In this example such a switch would be inconclusive and we must rely on the spectroscopic measurements for the assignment.

Summary

We have shown that the azide ion reacts rapidly and quantitatively with ruthenium carbonyl clusters, generating several new complexes containing the isocyanate ligand. The initial reaction solution of $Ru_3(CO)_{12}$ and N_3^- contains both $[Ru_3(NCO)(CO)_{11}]^-$ (the proposed initial product) and $[Ru_3(NCO)(CO)_{10}]^-$. These two trimeric clusters readily interconvert by the addition of or removal of carbon monoxide. Protonation of this reaction solution allows the isolation of $HRu_3(NCO)(CO)_{10}$ in low yield. Further reaction of $[Ru_3(NCO)(CO)_{10}]^-$ leads to the tetranuclear cluster $[Ru_4(NCO)(CO)_{13}]^-$, which can be isolated in overall 70% yield from $Ru_3(CO)_{12}$. Under a CO atmosphere $[Ru_4(NCO)(CO)_{13}]^-$ cleanly reverts back to $[Ru_3(NCO)(CO)_{11}]^-$ and $Ru_3(CO)_{12}$. When $[Ru_4(NCO)(CO)_{13}]^-$ is placed under a H_2 atmosphere, rapid substitution occurs, giving $[H_2Ru_4(NCO)(CO)_{12}]^-$, which can subsequently be protonated, forming $H_3Ru_4(NCO)(CO)_{12}$.

A general observation regarding this chemistry is the remarkable facility by which all of these clusters react. It would appear that the isocyanate ligand is somehow quite effective at labilizing both the metal–ligand and the metal–metal bonds. Whether this is unique to NCO^- or common to all halide- and pseudohalide-containing clusters is not yet known. In this light it is interesting to point out that many of the CO/H_2 reactions catalyzed by many carbonyls (in particular those of ruthenium) are promoted by halide ions.[26]

Acknowledgment. We gratefully acknowledge the National Science Foundation (Grant No. CHE 8106096) and Union Carbide Corp. for support of this work. We also thank Doyle Britton for assistance with the X-ray study.

Note Added in Proof. The product resulting from the pyrolysis of the trinuclear isocyanato clusters is $[Ru_6N(CO)_{16}]^-$. Details of this have been reported in: Blohm, M. L.; Fjare, D. E.; Gladfelter, W. L. *Inorg. Chem.* **1983**, *22*, 1004–1006.

Registry No. **7**, 85337-22-0; **12**, 84848-99-7; **13**, 85337-20-8; **15**, 85337-21-9; $Ru_3(CO)_{12}$, 15243-33-1; $H_2Ru_4(CO)_{13}$, 21077-76-9; $PPN(N_3)$, 38011-36-8.

Supplementary Material Available: Listings of the atomic coordinates and thermal parameters and the observed and calculated structure factors and a stereoview of the molecule (17 pages). Ordering information is given on any current masthead page.

(25) Johnson, B. F. G.; Lewis, J.; Raithby, P. R.; Sheldrick, G. M.; Wong, K.; McPartlin, M. *J. Chem. Soc., Dalton Trans.* **1978**, 673.

(26) (a) Dombek, B. D. *J. Am. Chem. Soc.* **1981**, *103*, 6508. (b) Knifton, J. F. *Ibid.* **1981**, *103*, 3959.